View Article Online / Journal Homepage / Table of Contents for this issue



# Photoinduced electron transfer of nanohybrids of carbon nanohorns with amino groups and tetrabenzoic acid porphyrin in aqueous media†

**Atula S. D. Sandanayaka,*[ab] Osamu Ito,*[a] Takatsugu Tanaka,[c] Hiroyuki Isobe,[d] Eiichi Nakamura,[c] Masako Yudasaka[e] and Sumio Iijima[e]**

*Received (in Montpellier, France) 16th July 2009, Accepted 3rd August 2009*
*First published as an Advance Article on the web 27th August 2009*
**DOI: 10.1039/b9nj00338j**

Published on 27 August 2009 on http://pubs.rsc.org | doi:10.1039/B9NJ00338J
Downloaded by University of Belgrade on 02 January 2013

Amino carbon nanohorns (**CNH**–$NH_2$) are covalently and non-covalently functionalized with tetrabenzoic acid porphyrin ($H_2P(CO_2H)_4$) forming dispersible nanohybrids in aqueous solution; the nanohybrids are characterized by spectroscopy and electron microscopy. Photoinduced electron-transfer processes of the nanohybrids of carbon nanohorns in aqueous solution are revealed with time-resolved absorption and fluorescence measurements. From the observed fluorescence quenching of the $H_2P(CO_2H)_4$ moieties by **CNH**–$NH_2$, charge separation *via* the excited singlet state of the $H_2P$ moieties, generating radical cations localized in the $H_2P$ moieties and electrons trapped in **CNH**, is suggested. In the presence of methylviologen dication ($MV^{2+}$) and a hole-shifting reagent, electron pooling is observed by the light-illumination of the $H_2P(CO_2H)_4$ moieties in **CNH**–$NH_2$ nanohybrids, suggesting that the electron generated by the charge-separation migrates to $MV^{2+}$ in aqueous solution.

## Introduction

Carbon-based nanostructured materials have been extensively investigated for their high potential in nanotechnological applications.[1] Among the various carbon nanomaterials, carbon nanohorns (**CNH**s) have emerged as an intriguing material.[2] In **CNH**s, horn-like carbons, which are single-graphene tubules with highly-strained conical-ends, are assembled to form dahlia-like spherical aggregates having diameters ranging between 50–100 nm.[2] One of the merits of **CNH**s different from other carbonaceous materials is a high carbon purity due to the absence of any metal nanoparticles, because of their synthetic procedure from highly purified graphite using laser ablation methods.[2] Thus, **CNH**s have attracted a great deal of attention; thus, various potential applications to gas storage, catalyst supports, drug carrier systems, and optoelectronic devices have been widely reported.[2]

Tagmatarchis *et al.* have succeeded in dispersing pristine **CNH**s with covalent and non-covalent attachments of various addends either onto the graphite-like side-walls or at the conical-shaped tips, which slightly perturbs the π-electronic network of **CNH**s.[3] Such treatments gave homogeneous **CNH**-solutions used for various fabrications opening up to the potential for wide applications.[3]

To mimic natural photosynthesis, nanohybrids consisting of carbon-based materials and porphyrin/phthalocyanine pigments are particularly promising.[4,5] Porphyrins and phthalocyanines act as light-harvesting antennae in a wide visible region.[6,7] The porphyrins and phthalocyanines form donor–acceptor nanohybrids with carbon nanomaterials; thus, porphyrins/phthalocyanines act as photosynthetic reaction centers after light absorption.[4–7] Recently, it has also been reported that the direct light excitation of the nanocarbon materials induces charge-separation;[8,9] the generated electrons on the nanocarbons transfer to the electrodes and holes transfer to the hole-transfer reagents in the solution, constructing photovoltaic cells.[8] Recently, it has been reported that light-illumination of the chemically attached chromospheres to **CNH**s induces the charge separation *via* the excited states of the chromospheres.[10] We also previously reported that the chemically modified **CNH**s are dispersible in organic solvents when the attached chromophores are soluble in organic solvents.[11] However, only a few studies have been reported for water soluble chemically modified **CNH**s,[12] although it is possible to evolve hydrogen gas under photo-illumination in the presence of an appropriate catalyst in aqueous solution, if the photoinduced charge-separated states persist for appropriately long times.[13,14]

In our previous study, we prepared **CNH**s with amino-groups (**CNH**–$NH_2$), by treatment with sodium amide in liquid ammonia.[15] The bonded amino groups covering the graphene surface are expected to make **CNH**–$NH_2$ hydrophilic,

[a] *Institute of Multidisciplinary Research for Advanced Materials, Tohoku University, Katahira, Sendai, 980-8577, Japan. E-mail: ito@tagen.tohoku.ac.jp*
[b] *School of Material Science, Japan Advanced Institute of Science and Technology, Asahidai, Nomi, 923-1292, Japan. E-mail: sandanay@jaist.ac.jp*
[c] *Department of Chemistry, The University of Tokyo, Hongo, Bunkyo-ku, Tokyo, 113-0033, Japan. E-mail: takatsugu@chem.s.u-tokyo.ac.jp, nakamura@chem.s.u-tokyo.ac.jp*
[d] *Department of Chemistry, Tohoku University, Aramaki, Aoba-ku, Sendai, 980-8576, Japan. E-mail: isobe@m.tains.tohoku.ac.jp*
[e] *Advanced Industrial Science and Technology, Central 5, 1-1-1 Higashi, Tsukuba, Ibaraki, 305-856, Japan. E-mail: s-iijima@aist.go.jp, m-yudasaka@aist.go.jp*

† Electronic supplementary information (ESI) available: Procedure of preparation, IR spectra, differential pulse voltammograms and nano-second transient absorption spectra. See DOI: 10.1039/b9nj00338j

Published on 27 August 2009 on http://pubs.rsc.org | doi:10.1039/B9NJ00338J
Downloaded by University of Belgrade on 02 January 2013

soluble in water, and supply chances of further functionalizations as a building block of nanohybrids with various chromospheres. In the present report, we functionalize **CNH**–$NH_2$ with free-base porphyrin with tetracarboxylic acids ($H_2P(CO_2H)_4$) to produce nanohybrids to investigate the light induced charge-separation processes.

## Results and discussion

To obtain nanohybrids of **CNH**–$NH_2$ having a high light-harvesting ability, $H_2P(CO_2H)_4$ was added to **CNH**–$NH_2$ in aqueous solution (Scheme 1), in which covalently and non-covalently attached nanohybrids are formed. Covalently bonded nanohybrids (**CNH**–NH–C(=O)–$H_2P(CO_2H)_3$) were shown to have amide bonds characterized by an IR band at 1665 $cm^{-1}$ (ESI, Fig. S1†). The presence of non-covalently attached nanohybrids (**CNH**–$NH_2$;$H_2P(CO_2H)_4$), in which both π-stacking and ionic bonding are effective, was also proven by the excess free carboxylic IR bands.

High-resolution transmission electron microscopy (HR-TEM) and dynamic light scattering (DLS) measurements have been used to probe the morphological characteristics and particle size distribution of the **CNH**–$NH_2$ and $H_2P(CO_2H)_4$-modified **CNH**–$NH_2$ nanohybrids. Typical HR-TEM images of the $H_2P(CO_2H)_4$-modified **CNH**–$NH_2$ nanohybrids are shown in Fig. 1(A) and (B). The carbon skeletons of nanohybrids look to be almost the same as untreated **CNH**–$NH_2$, indicating that the treatments of $H_2P(CO_2H)_4$ do not much affect the structures of **CNH**–$NH_2$; *i.e.*, the dahlia-like structures and the tips of the horns were kept without destruction, suggesting that $H_2P(CO_2H)_4$ molecules react and adsorb at the top of the horns and surfaces of **CNH**–$NH_2$. In addition, the average diameters of the **CNH**–$NH_2$ and $H_2P(CO_2H)_4$-modified **CNH**–$NH_2$ are estimated by DLS to be around 280 and 295 nm (Fig. 1(C) and (D)). The average diameter was found to be higher for $H_2P(CO_2H)_4$-modified **CNH**–$NH_2$, indicating that the nanohybrids tend to aggregate after treatments of $H_2P(CO_2H)_4$.

The functionalization of the $H_2P(CO_2H)_4$-modified **CNH**–$NH_2$ nanohorns was confirmed by thermogravimetric analysis (TGA). The TGA curves in Fig. 2 show that **CNH** (curve ii) and **CNH**–$NH_2$ (curve iii) demonstrate excellent thermal stability up to about 600 °C; at further high temperatures,

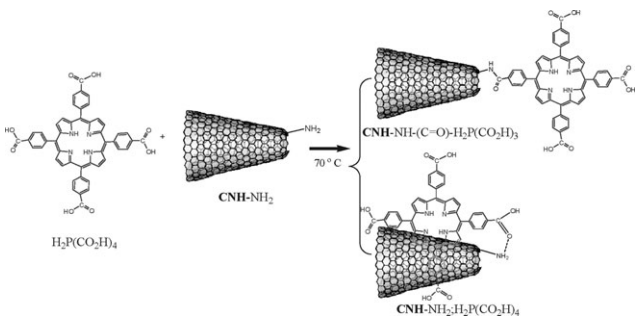


**Scheme 1** Nanohybrids of **CNH**–$NH_2$ with $H_2P(CO_2H)_4$ in alkali aqueous solution, which contains a mixture of covalent nanohybrid (**CNH**–NH–C(=O)–$H_2P(CO_2H)_n$ ($n$ = 3)) and non-covalent nanohybrid (**CNH**–$NH_2$;$H_2P(CO_2H)_4$).

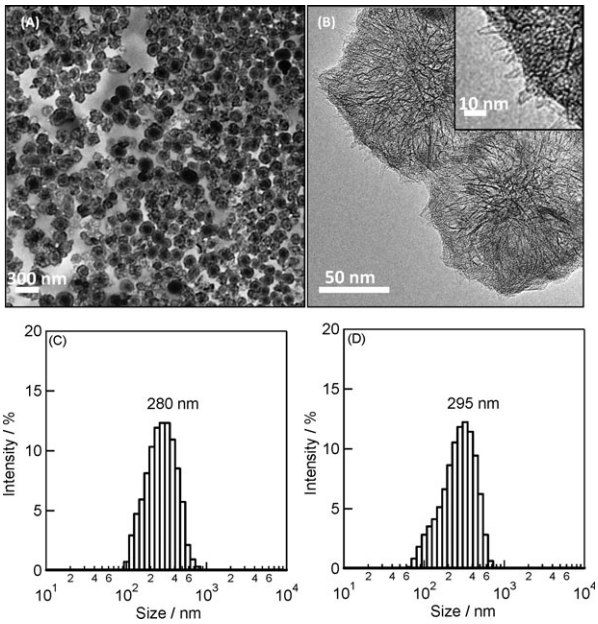


**Fig. 1** HR-TEM images of **CNH**–$NH_2$ nanohybrids obtained by treatment with $H_2P(CO_2H)_4$ (A and B (magnified scale)). Dynamic light scattering (DLS) measurement (C) **CNH**–$NH_2$ and (D) $H_2P(CO_2H)_4$ treated **CNH**–$NH_2$ nanohybrids.

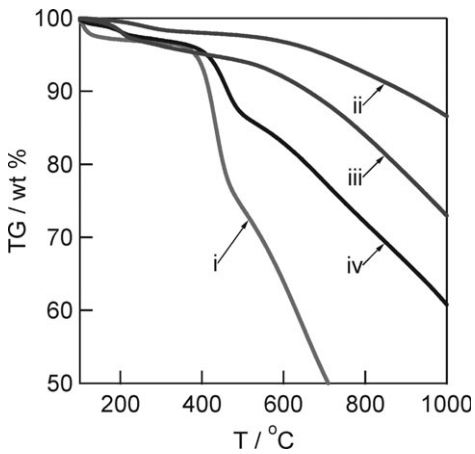


**Fig. 2** Thermogravimetric analyses obtained by treatment under $N_2$ atmosphere with 10 °C $min^{-1}$. (i) $H_2P(CO_2H)_4$, (ii) pristine **CNH**, (iii) **CNH**–$NH_2$, and (iv) $H_2P(CO_2H)_4$ nanohybrids with **CNH**–$NH_2$.

they exhibit monotonous and continuous weight loss of about 30% up to 1000 °C. Fig. 2 curve iv for $H_2P(CO_2H)_4$-modified **CNH**–$NH_2$ shows weight loss of about 10% at 450 °C due to decomposition of $H_2P(CO_2H)_4$ as compared with curve i for an $H_2P(CO_2H)_4$ molecule, showing rapid decrease at 430 °C of about 20%. Such differences support that considerable amounts of $H_2P(CO_2H)_4$ molecules are covalently and non-covalently attached to the **CNH**–$NH_2$ with considerable bonding energies. Thus, TGA results show that $H_2P(CO_2H)_4$-modified **CNH**–$NH_2$ nanohybrids, which are stable up to 450 °C, have been formed.

A steady-state absorption spectrum of the mixture of the covalent and non-covalent nanohybrids in aqueous solution is shown in Fig. 3(A) (spectrum iii) with the spectra of the

 This journal is © The Royal Society of Chemistry and the Centre National de la Recherche Scientifique 2009

components (spectrum i for $H_2P(CO_2H)_4$ and spectrum ii for **CNH**–$NH_2$). A sharp absorption at 420 nm due to the Soret-band of the $H_2P$ moiety (spectrum i) overlaps with featureless bands in the UV-visible and near-IR regions of **CNH**–$NH_2$ (spectrum ii).[15] However, slight red-shifts with band-broadenings were observed for the Soret-band and Q-band (520–620 nm) of the $H_2P$ moiety in nanohybrids, suggesting a π–π weak interaction of the $H_2P$ moieties with π-electron networks on the surface of **CNH**s for nanohybrids.

With the light-excitation of the $H_2P$ moieties in these nanohybrids, the steady-state fluorescence band appeared at 650 nm with a shoulder at 700 nm as shown in Fig. 3(B). Compared with $H_2P(CO_2H)_4$ (spectrum i), the fluorescence peak position of $H_2P(CO_2H)_4$-modified **CNH**–$NH_2$ nanohybrids shifts to a longer wavelength region by *ca.* 10 nm keeping the bandwidth (spectrum ii), suggesting the presence of weakly interacting excited $H_2P$ ($^1H_2P^*$) moieties with **CNH**–$NH_2$ in a mixture solution.

When the steady-state fluorescence intensities are measured with the same absorption intensity (ESI, Fig. S2†) of the $H_2P$ moiety at 420 nm, about 70% of $H_2P$-fluorescence intensity was quenched by **CNH**–$NH_2$ as shown in Fig. 3(B), which affords evidence of the formation of the nanohybrids between $H_2P(CO_2H)_4$ and **CNH**–$NH_2$. This $H_2P$-fluorescence-intensity

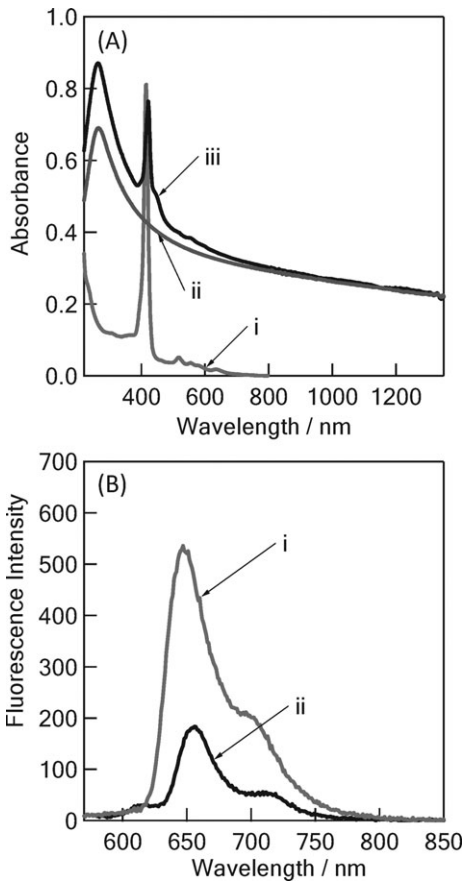


**Fig. 3** (A) Steady-state absorption spectra of (i) $H_2P(CO_2H)_4$ (0.01 mM) and (ii) **CNH**–$NH_2$; (iii) $H_2P(CO_2H)_4$ nanohybrids with **CNH**–$NH_2$ in aqueous solution and (B) fluorescence spectra of (i) $H_2P(CO_2H)_4$ (0.004 mM) and (ii) nanohybrids; the absorbance is normalized at $\lambda_{ex}$ = 420 nm.

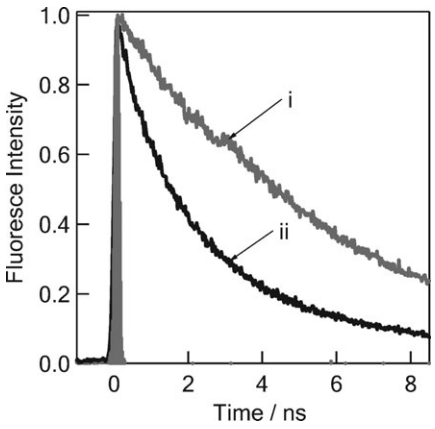


**Fig. 4** Fluorescence decays of (i) $H_2P(CO_2H)_4$ (0.01 mM) and (ii) $H_2P(CO_2H)_4$ nanohybrids with **CNH**–$NH_2$ in the 620–720 nm region in aqueous solution; $\lambda_{ex}$ = 400 nm.

quenching is usually caused by the photophysical events in the excited singlet state of the $H_2P$ moiety in the vicinity of **CNH**–$NH_2$ such as by a charge-separation process.

The fluorescence–time-profiles of the $H_2P$ moiety in the nanohybrid solution, measured by the excitation with a picosecond pulsed laser light at 400 nm, and the monitored fluorescence in the 620–720 nm region by streak-scope are shown in Fig. 4. The shortening of the fluorescence lifetime of the $H_2P$ moiety in the **CNH**–$NH_2$ nanohybrid was observed. From the curve-fitting with bi-exponential function, the fluorescence lifetimes of the $H_2P$ moiety were evaluated to be 1440 ps (65%) and 5200 ps (35%), which are shorter than the lifetime of unbound $H_2P(CO_2H)_4$ (7500 ps (100%)). These observations indicate an efficient deactivation process of $^1H_2P^*$ moiety by **CNH**–$NH_2$ in the nanohybrids, in agreement with the steady-state fluorescence-intensity quenching.

The rate constant ($k_q^F$) and the quantum yield ($\phi_q^F$) of fluorescence quenching were evaluated from the shorter fluorescence-lifetime component by the difference from that of unbound reference porphyrin.[16] The $k_q^F$ value was obtained to be $5.7 \times 10^8$ $s^{-1}$ and the $\phi_q^F$ value was 0.81 ($\phi_q^F$ × fraction = 0.53), suggesting a moderately efficient quenching process of $^1H_2P^*$. On the other hand, a longer fluorescence-lifetime component gave the $k_q^F$ value to be $5.9 \times 10^7$ $s^{-1}$. A faster quenching process corresponds to the closer contacting structures of $H_2P(CO_2H)_4$ with **CNH**–$NH_2$, since the closer contacting structures are expected both from the covalent bonding with π–π interaction (see lower structure in Scheme 1) and from non-covalent π–π stacking.

Electrochemical data also give information about the thermodynamics of the free-energy changes for the electron-transfer processes. In order to confirm broad peak positions in the cyclic voltammogram of the nanohybrids, differential pulsed voltammetry measurements were performed (ESI, Fig. S3†). A peak at 0.67 V *vs.* Ag/AgCl was observed for a solution of $H_2P(CO_2H)_4$ nanohybrids with **CNH**–$NH_2$, which was attributed to the first oxidation potential of the $H_2P$ moiety,[6] whereas two broad peaks in the negative potential region (−0.28 and −0.51 V *vs.* Ag/AgCl) may be attributed to the reduction potentials of **CNH**–$NH_2$[9,10] as comparing with $H_2P(CO_2H)_4$ monomer (0.76 V *vs.* Ag/AgCl) and **CNH**–$NH_2$

Published on 27 August 2009 on http://pubs.rsc.org | doi:10.1039/B9NJ00338J
Downloaded by University of Belgrade on 02 January 2013

Published on 27 August 2009 on http://pubs.rsc.org | doi:10.1039/B9NJ00338J
Downloaded by University of Belgrade on 02 January 2013

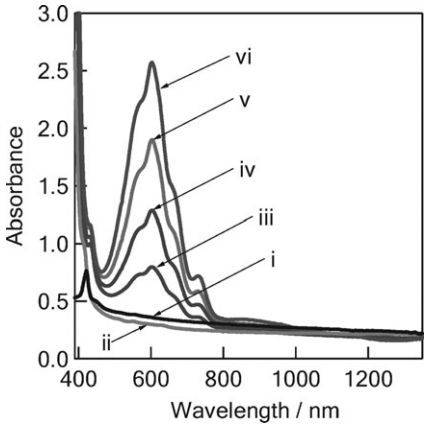


**Fig. 5** Steady-state absorption spectral changes observed after repeated 532 nm laser light irradiation of (i) the $H_2P(CO_2H)_4$ nanohybrids with **CNH**–$NH_2$; (ii) in the presence of $MV^{2+}$ (0.5 mM) without BNAH and (iii–vi) with BNAH: concentration of BNAH = (iii) 0.5, (iv) 1.0, (v) 1.5, and (vi) 2.0 mM in deaerated $H_2O$ (0.5 cm cell length).

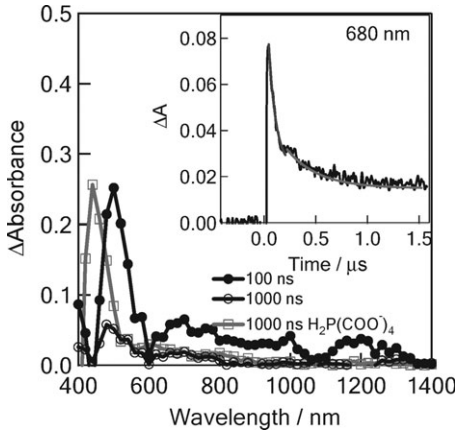


**Fig. 6** Nanosecond transient absorption spectra of nanohybrids between **CNH**–$NH_2$ and $H_2P(CO_2H)_4$ (●, ○) and $H_2P(CO_2H)_4$ (□) observed by 532 nm laser light irradiation in aqueous solution; spectra at 100 ns (●) and 1000 ns (○, □). Inset: absorption–time profiles at 680 nm of nanohybrids.

(−0.30 and 0.51 V *vs.* Ag/AgCl). The difference between the first oxidation potential and the first reduction potential gave the energy of charge-separated states to be in the region of 1.0–1.2 eV, from which the free energy changes of charge-separation *via* $^1H_2P^*$ (2.0 eV)[6] were evaluated to be −0.8 – −1.0 eV, suggesting that charge-separation processes are sufficiently exothermic *via* the $^1H_2P^*$ moiety in the $H_2P(CO_2H)_4$ nanohybrids with **CNH**–$NH_2$.

To confirm the charge-separation in the $H_2P(CO_2H)_4$ nanohybrids with **CNH**–$NH_2$, the steady-state absorption spectra were measured during the light irradiation of the nanohybrids in the presence of excess methyl viologen dication ($MV^{2+}$) as shown in Fig. 5. Only when 1-benzyl-1,4-dihydronicotinamide (BNAH) was added as a sacrificial hole shifter,[17] accumulation of methyl viologen radical cation ($MV^{\bullet+}$) was confirmed by the characteristic band at 620 nm as a result of the electron pooling. From the observed absorbance at 620 nm, the maximal concentration of $MV^{\bullet+}$ was found to be 0.39 mM, from which the conversion was evaluated to be 77% *vs.* the feed $MV^{2+}$ (0.5 mM). With an increase in the BNAH concentration, amounts of $MV^{\bullet+}$ increased indicating that back electron transfer from electron rich $MV^{\bullet+}$ to $H_2P^{\bullet+}$ was suppressed by hole shift from $H_2P^{\bullet+}$ to BNAH. After the hole shift, BNAH changes to $BNAH^{\bullet+}$, which spontaneously dissociates to 1-benzyl nicotinamide cation ($BNA^+$).

As control experiments in the absence of BNAH, no absorption of $MV^{\bullet+}$ was accumulated even after the laser-light irradiation of the $H_2P(CO_2H)_4$ nanohybrids with **CNH**–$NH_2$. Only a small amount of $MV^{\bullet+}$ accumulation (absorbance = 0.1 at 620 nm) was observed with the laser-light irradiation of $H_2P(CO_2H)_4$ without **CNH**–$NH_2$, suggesting that direct photoinduced electron transfer from $^1H_2P^*$ (or $^3H_2P^*$) to $MV^{2+}$ does not contribute to the accumulation of $MV^{\bullet+}$ without **CNH**–$NH_2$ (see ESI, Fig. S4†).

In order to reveal the transfer and migration mechanisms of electron and hole, the transient absorption spectra were observed upon excitation of the $H_2P$ moiety of the $H_2P(CO_2H)_4$ nanohybrids with **CNH**–$NH_2$ with 532 nm laser light as shown in Fig. 6, in which the transient absorption spectrum of unbound $H_2P(CO_2H)_4$ is also shown for comparison. The 450 nm band observed upon excitation of the unbound $H_2P(CO_2H)_4$ can be attributed to $^3H_2P^*$ (ESI, Fig. S5†). In the $H_2P(CO_2H)_4$ nanohybrids with **CNH**–$NH_2$, a clear band was observed at 500 nm with almost the same band shape to the unbound $^3H_2P^*$; thus, the 500 nm band can be attributed to the $^3H_2P^*$ bound to **CNH**–$NH_2$. Such a 50 nm shift suggests a considerably strong π–π interaction.

The decay rate of the 500 nm band was accelerated compared with the unbound $^3H_2P^*$ moiety (see ESI, Fig. S6†), indicating that quenching of $^3H_2P^*$ takes place on the surface of **CNH**–$NH_2$ ($k_{decay} = 2.0 \times 10^6\ s^{-1}$), suggesting that some photochemical events take place between two bound species. Newly observed transient absorption bands in the 640–720 nm region with a maximum at 680 nm can be attributed to the $H_2P^{\bullet+}$ moiety.[6]

The absorption bands in the 750–1300 nm region can be thought to be due to trapped electrons in the **CNH**–$NH_2$ as counterparts of the $H_2P^{\bullet+}$ moiety, since similar broad absorption bands were observed for the trapped electrons in **CNH** in our previous papers;[11,12] that is, such broad bands in the near-IR region are also due to trapped electrons, taking the complicated π-electron structures of **CNH** into consideration.

The time profile at 680 nm is shown in the inset of Fig. 6; the decay at 680 nm was curve-fitted by a bi-exponential function, giving the first-order rate constants to be $1.0 \times 10^7$ and $7.0 \times 10^5\ s^{-1}$. These rate constants can be attributed to the intra-nanohybrid charge-recombination ($k_{CR}$); larger $k_{CR}$ values are due to **CNH**$^{\bullet-}$–NH–C(=O)–$H_2P^{\bullet+}(CO_2H)_n$ ($n \leq 3$) and **CNH**$^{\bullet-}$–$NH_2$;$H_2P^{\bullet+}(CO_2H)_4$, generated *via* $^1H_2P^*$. Indeed, the decay at 1200 nm giving $k_{CR} = 1.0 \times 10^7\ s^{-1}$ corresponds to the faster decay at 680 nm, supporting the charge recombination process. On the other hand, smaller $k_{CR}$ values may be attributed to the charge-recombination of the radical ion pairs generated *via* a $^3H_2P^*$ moiety.

On addition of $MV^{2+}$ to $H_2P(CO_2H)_4$ nanohybrids with **CNH**–$NH_2$, the transient spectra showed a new peak in the

 This journal is © The Royal Society of Chemistry and the Centre National de la Recherche Scientifique 2009

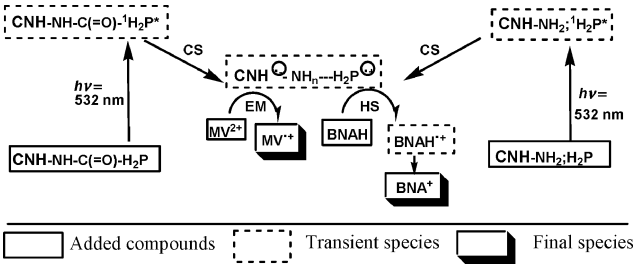


**Scheme 2** Schematic representation for electron-transfer/electron-mediation/hole-shift processes of nanohybrids containing both **CNH**–NH–C(=O)–$H_2P(CO_2H)_n$ ($n \leq 3$) and **CNH**–$NH_2$;$H_2P(CO_2H)_4$ in aqueous solution; only the excited singlet state route is shown and carboxylic acids are omitted for simplicity.

580–680 nm region with a maximum at 620 nm due to $MV^{\bullet+}$ with concomitant decrease of the near-IR bands (ESI, Fig. S7;† the 1200 nm absorption intensity decreased from 0.12 to 0.04 immediately after laser light pulse), suggesting that electron migration occurs from the **CNH**$^{\bullet-}$-moiety to $MV^{2+}$.[18] This observation also confirms that the decreased broad transient absorption bands in the whole near-IR region are due to **CNH**$^{\bullet-}$.[11,12] When both BNAH and $MV^{2+}$ were added to nanohybrid solutions, the transient absorption band of $MV^{\bullet+}$ persists without decay until a few hundred microseconds, indicating that back electron transfer from electron rich $MV^{\bullet+}$ to positive species (predominantly the $H_2P^{\bullet+}$ moiety) was almost completely suppressed by hole shift from $H_2P^{\bullet+}$ to BNAH, which is a well-known irreversible hole trap.[17]

These observations for $H_2P(CO_2H)_4$ nanohybrids with **CNH**–$NH_2$ can be explained by the processes summarized in Scheme 2, in which charge-separation initially takes place *via* the $^1H_2P^*$–$^3H_2P^*$ moiety, generating the radical ion pairs such as **CNH**$^{\bullet-}$–NH–C(=O)–$H_2P^{\bullet+}(CO_2H)_n$ ($n \leq 3$) and **CNH**$^{\bullet-}$–$NH_2$;$H_2P^{\bullet+}(CO_2H)_4$ in alkaline aqueous solution. Thus, the shorter fluorescence lifetime is attributed to the charge-separation within nanohybrids *via* $^1H_2P^*$. The $k_q^F$ and $\phi_q^F$ are corresponding to those of the charge-separation; that is, $k^S_{CS} = 5.7 \times 10^8\ s^{-1}$ and $\phi^S_{CS} = 0.81$, suggesting a moderately efficient charge-separation process *via* $^1H_2P^*$; the $k_{CR}$ value is $1.0 \times 10^7\ s^{-1}$. In the case of $^3H_2P^*$, $k^T_{CS} = 2.0 \times 10^6\ s^{-1}$ and the corresponding $k_{CR} = 7.0 \times 10^5\ s^{-1}$. On addition of $MV^{2+}$ and BNAH, the electrons on **CNH** mediate to $MV^{2+}$, accumulating $MV^{\bullet+}$. These processes are all exothermic to proceed efficiently (Scheme 2).

## Conclusions

In summary, we have shown a good example of a photo-induced charge-separation process of water-soluble **CNH**–$NH_2$ connected covalently and non-covalently with carboxylated porphyrins. By the direct excitation of the porphyrin moiety in the nanohybrids (**CNH**–$NH_2$;$H_2P(CO_2H)_4$ and **CNH**–NH–C(=O)–$H_2P(CO_2H)_n$ ($n \leq 3$)), generation of a charge-separated state, $H_2P^{\bullet+}$ and **CNH**$^{\bullet-}$, *via* the excited singlet and triplet states of the $H_2P$ moiety was confirmed. Since $H_2P^{\bullet+}$ and **CNH**$^{\bullet-}$ persist in longer time than 100–500 ns, they have enough time to mediate an electron on **CNH** to $MV^{2+}$ and concomitantly to shift a hole of $H_2P$ to BNAH. Thus, accumulation of $MV^{\bullet+}$ as an electron pool was observed by the light irradiation of a mixture of $H_2P(CO_2H)_4$ nanohybrids with **CNH**–$NH_2$ in the presence of a sacrificial hole shifter. Usually, the accumulated $MV^{\bullet+}$ can be further used as an electron source transferring to electrodes for a photovoltaic cell and to catalyses for $H_2$-evolution in aqueous solution. Such studies aiming applications to biosensing have been recently reported.[19]

## Experimental section

### Chemicals

Commercially available 4,4′,4″,4‴-(porphine-5,10,15,20-tetrayl)-tetrakis(benzoic acid), which is abbreviated as $H_2P(CO_2H)_4$, was purchased from Aldrich Chemicals (Milwaukee, WI) and was used as received.

### Sample preparation

**CNH**s used in the present study were produced by $CO_2$ laser ablation of graphite in the absence of any metal catalyst under an Ar atmosphere at room temperature; the purity of **CNH**s was as high as 90%.[2] **CNH**–$NH_2$ was prepared by the reaction of **CNH**s with sodium amide in liquid ammonia according to the previously reported method.[15] In order to obtain nanohybrids, $H_2P(CO_2H)_4$ was added to the **CNH**–$NH_2$ aqueous solution, and the mixture was heated to give homogeneous nanohybrid aqueous solution (see ESI, Scheme S1†). Covalent amide bonds were proven by the IR characteristic band (ESI, Fig. S1†).

### Instrumentation

High-resolution transmission electron microscopy (HR-TEM) measurements were carried out using a 002B Topcon operated at an accelerating voltage of 120 kV for imaging. The particle size and distribution were measured in aqueous suspension, using light scattering equipment (Zetasizer nano ZS). The thermogravimetric analysis was performed using a Perkin Elmer TGA 7 instrument in an inert atmosphere of nitrogen and helium. In a typical experiment 10 mg of the material was placed in the sample pan and the temperature was equilibrated at 150 °C. Subsequently, the temperature was increased to 1000 °C at a rate of 10 °C $min^{-1}$ and the weight changes were recorded as a function of temperature.

Steady-state absorption spectra in the visible and near-IR regions were measured on a JASCO V570 DS spectrometer. Steady-state fluorescence spectra were measured on a Shimadzu RF-5300PC spectrofluorophotometer. The picosecond time-resolved fluorescence spectra and the time profiles were measured using an argon-ion pumped Ti:sapphire laser (Tsunami) and a streak scope (Hamamatsu Photonics). The details of the experimental setup are described elsewhere.[20] Nanosecond transient absorption spectra in the visible and near-IR region were measured by means of laser-flash photolysis; pulsed light from a Nd:YAG laser (*ca.* 3 mJ per pulse) was used as an exciting source and Si- and Ge-avalanche photodiode modules were used for detecting the monitoring light from a pulsed Xe-lamp as described in our previous reports.[20]

Published on 27 August 2009 on http://pubs.rsc.org | doi:10.1039/B9NJ00338J
Downloaded by University of Belgrade on 02 January 2013

View Article Online

Published on 27 August 2009 on http://pubs.rsc.org | doi:10.1039/B9NJ00338J
Downloaded by University of Belgrade on 02 January 2013

The cyclic voltammetry and differential pulse voltammetry measurements were performed on a BAS CV-50 W electrochemical analyzer in deaerated aqueous solution containing 0.1 M KCl as a supporting electrolyte at a scan rate of 100 mV $s^{-1}$. The measured potentials were recorded with respect to an Ag/AgCl electrode (saturated with KCl).

## Acknowledgements

The authors thank Dr J. Fan of NEC for the HR-TEM measurements, and Dr T. Hasobe of Japan Advance Institute of Science and Technology (Kanazawa) for the IR measurements.

## References

1 P. M. Ajayan, *Chem. Rev.*, 1999, **99**, 1787; M. S. Dresselhaus, G. Dresselhaus and P. Avouris, *Carbon Nanotubes: Synthesis, Structure, Properties and Applications*, Springer-Verlag, Heidelberg, 2001, vol. 80; S. Reich, C. Thomsen and J. Maultzsch, *Carbon Nanotubes: Basic Concepts and Physical Properties*, Wiley-VCH, Weinheim, 2004; M. Meyyappan, *Carbon Nanotubes: Science and Applications*, CRC Press, Washington, D.C., New York, 2005.

2 For CHNs, see: S. Iijima, M. Yudasaka, R. Yamada, S. Bandow, K. Suenaga, F. Kokai and K. Takahashi, *Chem. Phys. Lett.*, 1999, **309**, 165; S. Iijima, *Phys. B*, 2002, **323**, 1; J. Fan, M. Yudasaka, Y. Kasuya, D. Kasuya and S. Iijima, *Chem. Phys. Lett.*, 2004, **397**, 5; K. Murata, A. Hashimoto, M. Yudasaka, D. Kasuya, K. Kaneko and S. Iijima, *Adv. Mater.*, 2004, **16**, 1520; H. Murakami, K. Ajima, J. Miyawaki, M. Yudasaka, S. Iijima and K. Shiba, *Mol. Pharm.*, 2004, **1**, 399.

3 N. Tagmatarchis, A. Maigne, M. Yudasaka and S. Iijima, *Small*, 2006, **2**, 490; G. Pagona, J. Fan, N. Tagmatarchis, M. Yudasaka and S. Iijima, *Chem. Mater.*, 2006, **18**, 3918.

4 For porphyrins non-covalently attached to carbon nanotubes, see: Y.-P. Sun, K. Fu, Y. Lin and W. Huang, *Acc. Chem. Res.*, 2002, **35**, 1096; H. Kataura, Y. Maniwa, M. Abe, A. Fujiwara, K. Kikuchi, H. Imahori, Y. Misaki, S. Suzuki and Y. Achiba, *Appl. Phys. A: Mater. Sci. Process.*, 2002, **74**, 349; H. Murakami, T. Nomura and N. Nakashima, *Chem. Phys. Lett.*, 2003, **378**, 481; S. Barazzouk, S. Hotchandani, K. Vinodgopal and P. V. Kamat, *J. Phys. Chem. B*, 2004, **108**, 17015; D. M. Guldi, H. Taieb, G. M. A. Rahman, N. Tagmatarchis and M. Prato, *Adv. Mater.*, 2005, **17**, 871; G. M. A. Rahman, D. M. Guldi, S. Campidelli and M. Prato, *J. Mater. Chem.*, 2006, **16**, 62; M. Alvaro, P. Atienzar, P. de la Cruz, J. L. Delgado, V. Troiani, H. Garcia, F. Langa, A. Palkar and L. Echegoyen, *J. Am. Chem. Soc.*, 2006, **128**, 6626; K. Schulte, J. C. Swarbrick, N. A. Smith, F. Bondino, E. Magnano and A. N. Khlobystov, *Adv. Mater.*, 2007, **19**, 3312.

5 For porphyrins covalently attached to carbon nanotubes, see: H. Li, R. B. Martin, B. A. Harruff, R. A. Carino and Y.-P. Sun, *Adv. Mater.*, 2004, **16**, 896; D. Baskaran, J. W. Mays, X. P. Zhang and M. S. Bratcher, *J. Am. Chem. Soc.*, 2005, **127**, 6916; Z. Guo, F. Du, D. Ren, Y. Chen, J. Zheng, Z. Liu and J. Tian, *J. Mater. Chem.*, 2006, **16**, 3021; B. Ballesteros, G. de la Torre, C. Ehli, G. M. Aminur-Rahman, F. Agulló-Rueda, D. M. Guldi and T. Torres, *J. Am. Chem. Soc.*, 2007, **129**, 5061; T. Umeyama, M. Fujita, N. Tezuka, N. Kadota, Y. Matano, K. Yoshida, S. Isoda and H. Imahori, *J. Phys. Chem. C*, 2007, **111**, 11484.

6 H. Imahori and Y. Sakata, *Adv. Mater.*, 1997, **9**, 537; D. M. Guldi and M. Prato, *Acc. Chem. Res.*, 2000, **33**, 695; M. E. El-Khouly, O. Ito, P. M. Smith and F. D'Souza, *J. Photochem. Photobiol., C*, 2004, **5**, 79; H. Imahori and S. Fukuzumi, *Adv. Funct. Mater.*, 2004, **14**, 525; F. D'Souza and O. Ito, *Coord. Chem. Rev.*, 2005, **249**, 1410; Y. Araki and O. Ito, *J. Photochem. Photobiol., C*, 2008, **9**, 93.

7 R. Chitta, A. S. D. Sandanayaka, A. L. Schumacher, L. D'Souza, Y. Araki, O. Ito and F. D'Souza, *J. Phys. Chem. C*, 2007, **111**, 6947.

8 D. M. Guldi, G. M. A. Rahman, N. Jux, N. Tagmatarchis and M. Prato, *Angew. Chem., Int. Ed.*, 2004, **43**, 5526; T. Hasobe, S. Fukuzumi and P. V. Kamat, *J. Am. Chem. Soc.*, 2005, **127**, 11884; T. Hasobe, S. Fukuzumi and P. V. Kamat, *Angew. Chem., Int. Ed.*, 2006, **45**, 975; T. Hasobe, S. Fukuzumi and P. V. Kamat, *J. Phys. Chem. B*, 2006, **110**, 25477; K. Saito, M. Ohtani and S. Fukuzumi, *J. Am. Chem. Soc.*, 2006, **128**, 14216.

9 A. S. D. Sandanayaka, Y. Takaguchi, T. Uchida, Y. Sako, Y. Morimoto, Y. Araki and O. Ito, *Chem. Lett.*, 2006, **35**, 1188; A. S. D. Sandanayaka, H. Orisaka, T. Kyotani, Y. Araki and O. Ito, *Carbon*, 2007, **45**, 684.

10 C. Cioffi, S. Campidelli, C. Sooambar, M. Marcaccio, G. Marcolongo, M. Meneghetti, D. Paolucci, F. Paolucci, C. Ehli, G. M. A. Rahman, V. Sgobba, V. D. M. Guldi and M. Prato, *J. Am. Chem. Soc.*, 2007, **129**, 3938.

11 A. S. D. Sandanayaka, G. Pagona, N. Tagmatarchis, M. Yudasaka, S. Iijima, Y. Araki and O. Ito, *J. Mater. Chem.*, 2007, **17**, 2540; G. Pagona, A. S. D. Sandanayaka, Y. Araki, J. Fan, N. Tagmatarchis, G. Charalambidis, P. Trohopoulos, A. G. Coutsolelos, B. Boitrel, M. Yudasaka, S. Iijima and O. Ito, *Adv. Funct. Mater.*, 2007, **17**, 1705; G. Rotas, A. S. D. Sandanayaka, N. Tagmatarchis, T. Ichihashi, M. Yudasaka, S. Iijima and O. Ito, *J. Am. Chem. Soc.*, 2008, **130**, 4725.

12 G. Pagona, A. S. D. Sandanayaka, Y. Araki, J. Fan, N. Tagmatarchis, M. Yudasaka, S. Iijima and O. Ito, *J. Phys. Chem. B*, 2006, **110**, 20729; G. Pagona, A. S. D. Sandanayaka, A. Maigné, J. Fan, G. C. Papavassiliou, I. D. Petsalakis, B. R. Steele, M. Yudasaka, S. Iijima, N. Tagmatarchis and O. Ito, *Chem.–Eur. J.*, 2007, **13**, 7600; M. Zhang, M. Yudasaka, T. Murakami, K. Ajima, A. S. D. Sandanayaka, O. Ito, K. Tsuchita and S. Iijima, *Proc. Natl. Acad. Sci. U. S. A.*, 2008, **105**, 14773; A. S. D. Sandanayaka, O. Ito, M. Zhang, K. Ajima, S. Iijima, M. Yudasaka, T. Murakami and K. Tsuchita, *Adv. Mater.*, DOI: 10.1002/adma.200901256.

13 P. Keller and A. Moradpour, *J. Am. Chem. Soc.*, 1980, **102**, 7193; P. Keller, A. Moradpour, E. Amouyel, H. Kagan and J. Mol. Catal, *J. Mol. Catal*, 1980, **7**, 539; A. I. Krasna, *Photochem. Photobiol.*, 1980, **31**, 75; J. M. Calvert, T. J. Manuccia and R. J. Nowak, *J. Electrochem. Soc.*, 1986, **133**, 951; R. J. McMahon, R. K. Force, H. H. Patterson and M. S. Wrighton, *J. Am. Chem. Soc.*, 1988, **110**, 2670; I. Okura, *Photosensitization of Porphryins and Phthalocyanines*, Gordon and Breach Science Publishers, Amsterdam, 2001.

14 P. M. S. Monk, *The Viologens*, John Wiley & Sons, Chichester, 1998.

15 R. Yuge, M. Yudasaka, J. Miyawaki, Y. Kubo, T. Ichihashi, H. Imai, E. Nakamura, H. Isobe, H. Yorimitsu and S. Iijima, *J. Phys. Chem. B*, 2005, **109**, 17861; J. Miyawaki, M. Yudasaka, H. Imai, H. Yorimitsu, H. Isobe, E. Nakamura and S. Iijima, *J. Phys. Chem. B*, 2006, **110**, 5179; H. Isobe, T. Tanaka, R. Maeda, E. Noiri, N. Solin, M. Yudasaka, S. Iijima and E. Nakamura, *Angew. Chem., Int. Ed.*, 2006, **45**, 6676.

16 $k_{CS} = (1/\tau_f)_{sample} - (1/\tau_f)_{ref}$ and $\Phi_{CS} = [(1/\tau_f)_{sample} - (1/\tau_f)_{ref}]/(1/\tau)_{sample}$; $\tau_{ref} = 7500$ ns.

17 S. Fukuzumi, S. Koumitsu, K. Hironaka and T. Tanaka, *J. Am. Chem. Soc.*, 1987, **109**, 305; S. Fukuzumi, H. Imahori, K. Okamoti, H. Yamada, M. Fujitsuka, O. Ito and D. M. Guldi, *J. Phys. Chem. A*, 2002, **106**, 1903.

18 The second-order rate constant for intermolecular electron transfer ($k_{second\text{-}order}$) as fast as a diffusion controlled limit ($k_{Diff}$) in the presence of $[MV^{2+}] = 0.5$ mM can be evaluated to be $5.9 \times 10^9$ $M^{-1}$ $s^{-1}$ from the observed $k_{first\text{-}order} = 3 \times 10^6$ $s^{-1}$. For $k_{Diff}$, see S. I. Murov, I. Carmichael and G. L. Hug, *Handbook of Photochemistry*, Marcel-Dekker, New York, 1993.

19 W.-W. Tu, J.-P. Lei, L. Ding and H.-X. Ju, *Chem. Commun.*, 2009, 4227.

20 Y. Araki and O. Ito, in *Handbook of Organic Electronics and Photonics*, ed. H. S. Nalwa, American Scientific Publishers, California, 2008, ch. 12, vol. 2, pp. 473–513.

 This journal is © The Royal Society of Chemistry and the Centre National de la Recherche Scientifique 2009